Non-smooth bifurcations in a double-scroll circuit with periodic excitation*

Zhang Yin(张 银) and Bi Qin-Sheng(毕勤胜)†

Faculty of Science, Jiangsu University, Zhenjiang 212013, *China*

(Received 7 May 2010; revised manuscript received 10 June 2010)

The fast-slow effect can be observed in a typical non-smooth electric circuit with order gap between the natural frequency and the excitation frequency. Numerical simulations are employed to show complicated behaviours, especially different types of busting phenomena. The bifurcation mechanism for the bursting solutions is analysed by assuming the forms of the solutions and introducing the generalized Jacobian matrix at the non-smooth boundaries, which can also be used to account for the evolution of the complicated structures of the phase portraits with the variation of the parameter. Period-adding bifurcation has been explored through the computation of the eigenvalues related to the solutions. At the non-smooth boundaries the so-called 'single crossing bifurcation' can occur, corresponding to the case where the eigenvalues jump only once across the imaginary axis, which leads the periodic burster to have a quasi-periodic oscillation.

Keywords: Matsumoto's circuit, non-smooth bifurcation, fast-slow effect, bursting

PACS: 05.45.Ac, 05.45.Pq **DOI:** 10.1088/1674-1056/20/1/010504

1. Introduction

Non-smooth factors may cause complicated behaviours in many dynamic systems, which attracts a lot of researchers to investigate the mechanism for the evolution to complexity.[1] Different types of non-conventional bifurcations, which are the combinations of several forms of conventional bifurcations, may occur when the phase trajectories pass across the non-smooth boundaries, leading to a variety of special dynamical characteristics.[2] Because of its easy implementation in real experiment, non-smooth electrical circuits are widely used to explore these nonlinear phenomena in non-smooth systems.[3] As a well-known non-smooth circuit, the Matsumoto's circuit, which can also be called Chua's circuit, has been studied by many researchers.[4] Several bifurcations have been reported in the simple Matsumoto's circuit with a piecewise-linear resistor or in the slightly modified versions of the circuit.[5,6] The phenomena such as period-doubling bifurcations to chaos, intermittence can be observed with the variation of parameters.[7] Furthermore, a well-known attractor in the literature, called the double-scroll attractor, can be found when the Matsumoto's electronic circuit is in a chaotic regime.[4]

The double-scroll circuit has been studied for its electronic simplicity and variety of non-smooth phenomena. The driven versions of this circuit have been extensively investigated by many authors who have found many bifurcation phenomena not to be observed in the non-perturbed circuit. These research activities resulted in a lot of publications on phenomena that such systems exhibit.[8,9]

Recently, many reports have focused on a special type of nonlinear system with two time scales, which often behaves in a periodic state characterized by a combination of relatively large amplitude and nearly harmonic small amplitude oscillation, conventionally called mixed-mode oscillation.[10,11] The fast–slow effect can be observed in many practical systems, such as artificial neural networks,[12] chemical reactions.[13]

The interaction between two time scales may cause the system to alternately reside between the quiescent state (QS) and the spiking state (SP), thereby forming different types of bursters. Two important bifurcations occur for the alternation in a burster, i.e., the bifurcation from the QS to SP and the bifurcation from SP to QS. The details for the bursters of the vector field with low dimension have been well summarized by Izhikevich.[14]

In many real electrical circuits, the fast–slow effect can also be observed when the vector fields are related to two time scales, which may lead to complicated behaviours, especially various kinds of bursters.

*Project supported by the National Natural Science Foundation of China (Grant Nos. 10972091 and 10872080).

†Corresponding author. E-mail: qbi@ujs.edu.cn

© 2011 Chinese Physical Society and IOP Publishing Ltd

Furthermore, most of the work related to electrical circuits is restricted to the autonomous cases. Here we focus our attention on the investigations of non-smooth circuit driven by periodic excitation and the dynamics when there exists order gap between the natural frequency and the excitation frequency in order to reveal the bursting phenomena as well as the associated bifurcation mechanism.

2. Double-scroll circuit with periodic excitation

The double-scroll circuit illustrated in Fig. 1(a) without w, which is established by Matsumoto and Chua,[4] is composed of two capacitors (C_1 and C_2), one inductor (L), a liner resistor represented by its admittance ($g = 1/R$), and a nonlinear resistor ($R_{\rm N}$), whose characteristic curve is presented in Fig. 1(b).

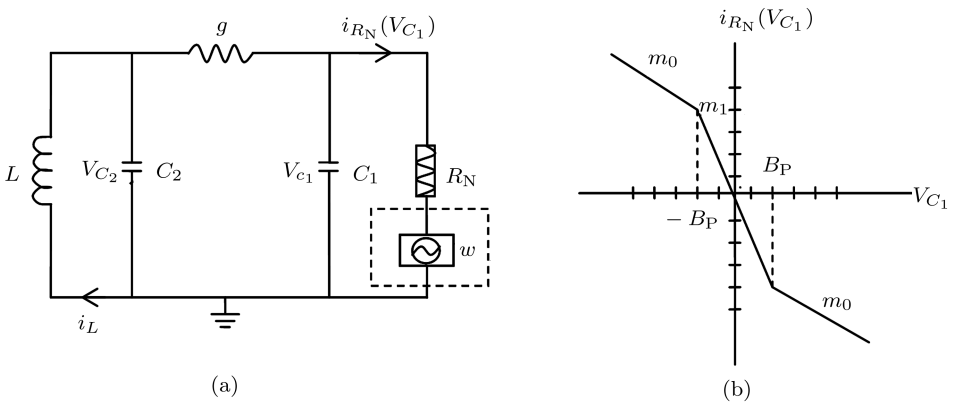


Fig. 1. (a) Schematic diagram of the double-scroll circuit and (b) characteristic curve of the nonlinear resistance $R_{\rm N}$.

Now we introduce a periodically changed electrical source w into the circuit, which is represented by

$$w = I_{\rm s}\cos(\Omega t), \tag{1}$$

where $I_{\rm s}$ and Ω represent the excitation amplitude and the excitation angular frequency, respectively.

From Fig. 1.(a), by applying Kirchoff's laws, the dynamics of the double-scroll circuit with periodic excitation can then be described by the following differential equations:

$$\begin{aligned}
\frac{{\rm d}V_{C_1}}{{\rm d}t} &= \frac{V_{C_2}-V_{C_1}}{RC_1} - \frac{i_{R_{\rm N}}(V_{C_1})}{C_1} + \frac{w}{C_1},\\
\frac{{\rm d}V_{C_2}}{{\rm d}t} &= \frac{V_{C_1}-V_{C_2}}{RC_2} + \frac{i_L}{C_2},\\
\frac{{\rm d}i_L}{{\rm d}t} &= -\frac{V_{C_2}}{L},
\end{aligned} \tag{2}$$

where V_{C_1} and V_{C_2} are the voltages across the capacitors C_1 and C_2, i_L and $i_{R_{\rm N}}$ are the electric currents passing through inductor L and $R_{\rm N}$, respectively. Furthermore, the current across the nonlinear resistance $R_{\rm N}$ can be presented by

$$i_{R_{\rm N}}(V_{C_1}) = m_0 V_{C_1} + \frac{1}{2}(m_1 - m_0) \times (|V_{C_1} + B_{\rm P}| - |V_{C_1} - B_{\rm P}|), \tag{3}$$

where m_0, m_1, and $B_{\rm P}$ are indicated in Fig. 1(b).

By introducing variables $x = V_{C_1}/B_{\rm P}$, $y = V_{C_2}/B_{\rm P}$, $z = i_L/gB_{\rm P}$, and $\tau = gt/C_2$, Eq. (2) can be written in the dimensionless form as

$$\begin{aligned}
\frac{{\rm d}x}{{\rm d}\tau} &= \alpha[y - x - k(x)] + w_0,\\
\frac{{\rm d}y}{{\rm d}\tau} &= x - y + z,\\
\frac{{\rm d}z}{{\rm d}\tau} &= -\beta y
\end{aligned} \tag{4}$$

with

$$k(x) = bx + \frac{1}{2}(a-b)(|x+1| - |x-1|), \tag{5}$$

$$w_0 = I\cos(\omega\tau), \tag{6}$$

where the new parameters are $\alpha = C_2/C_1$, $\beta = C_2/Lg^2$, $a = m_1/g$, $b = m_0/g$, $I = C_2 I_{\rm s}/gB_{\rm P}C_1 = \alpha I_{\rm s}/gB_{\rm P}$ and $\omega = C_2\Omega/g$.

3. Numerical simulations

Here we use the dimensionless parameters rather than their original physical quantities, for clarity, to investigate the behaviour of system (4). For the parameters fixed at $I = 0.2$, $\omega = 0.05$, $\alpha = 1.0$, $a = -8.0/7.0$, $b = -5.0/7.0$, the dynamical evolution of Eq. (4) with the variation of β is plotted in Fig. 2.

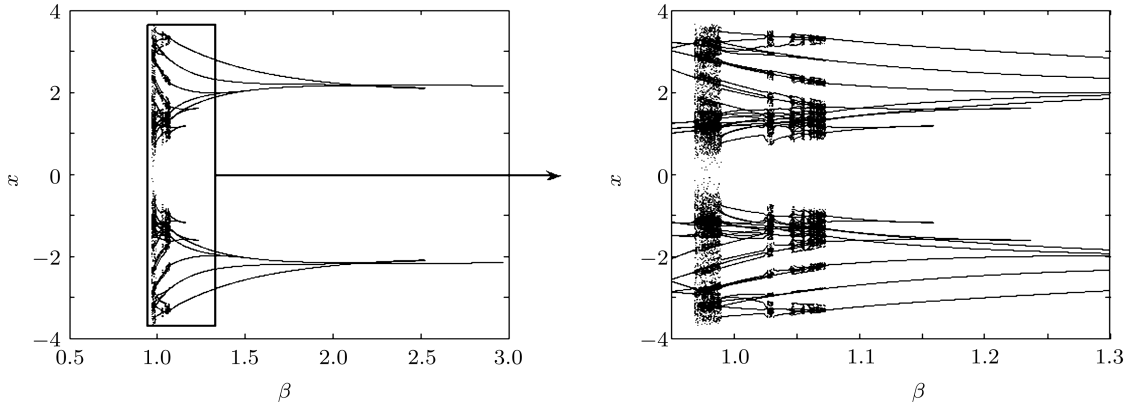


Fig. 2. Bifurcation diagram of system (4) with variation of β.

Periodic oscillations can be observed for relatively large values of β. For example, when $\beta = 2.0$, periodic movement with mixed mode oscillation can be found (shown in Fig. 3). The combination of large-amplitude oscillation associated with the excitation frequency and the small-amplitude oscillation corresponding to the natural frequency forms the L^S oscillation in the circuit, where L and S are corresponding to the multiples of the large-amplitude and the small-amplitude oscillation during one period respectively.[15]

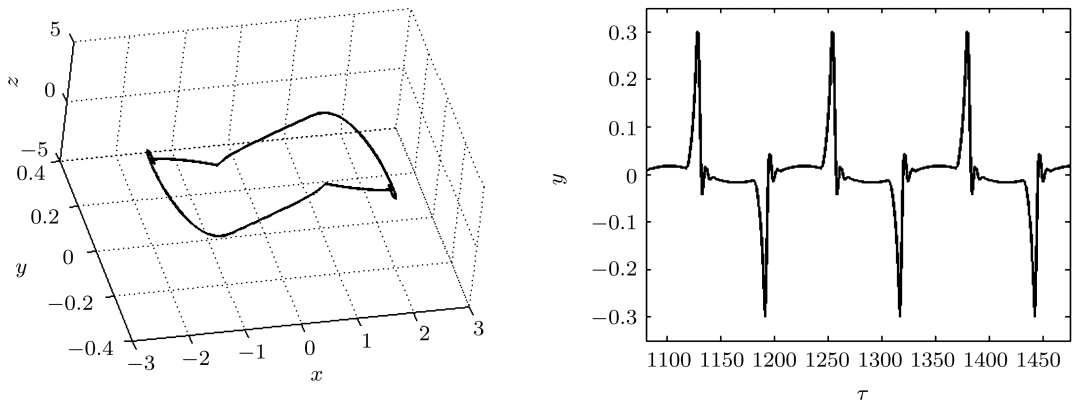


Fig. 3. Phase portraits and time variation of system (4) for $\beta = 2.0$.

Note that the period of the motion is the same as that of the excitation. Furthermore, during each period, small-amplitude oscillations around two symmetric sets can be observed, while large-amplitude oscillations occur when the trajectory moves between the oscillations near the two sets.

A sequence of period-adding bifurcations associated with the natural frequency occurs with the decrease of β, though the period of the movement is almost the same, which implies that S increases quickly for the L^S solution (see Fig. 4).

The periodic L^S mixed mode oscillation loses the stability at $\beta = 0.96$, leading to a quasi-periodic oscillation (see Fig. 5). Both the amplitude and the time needed for the small-amplitude oscillation increase quickly to cover the whole time variation of the attractor, though there still exists a great difference between the two frequencies involving in the solution.

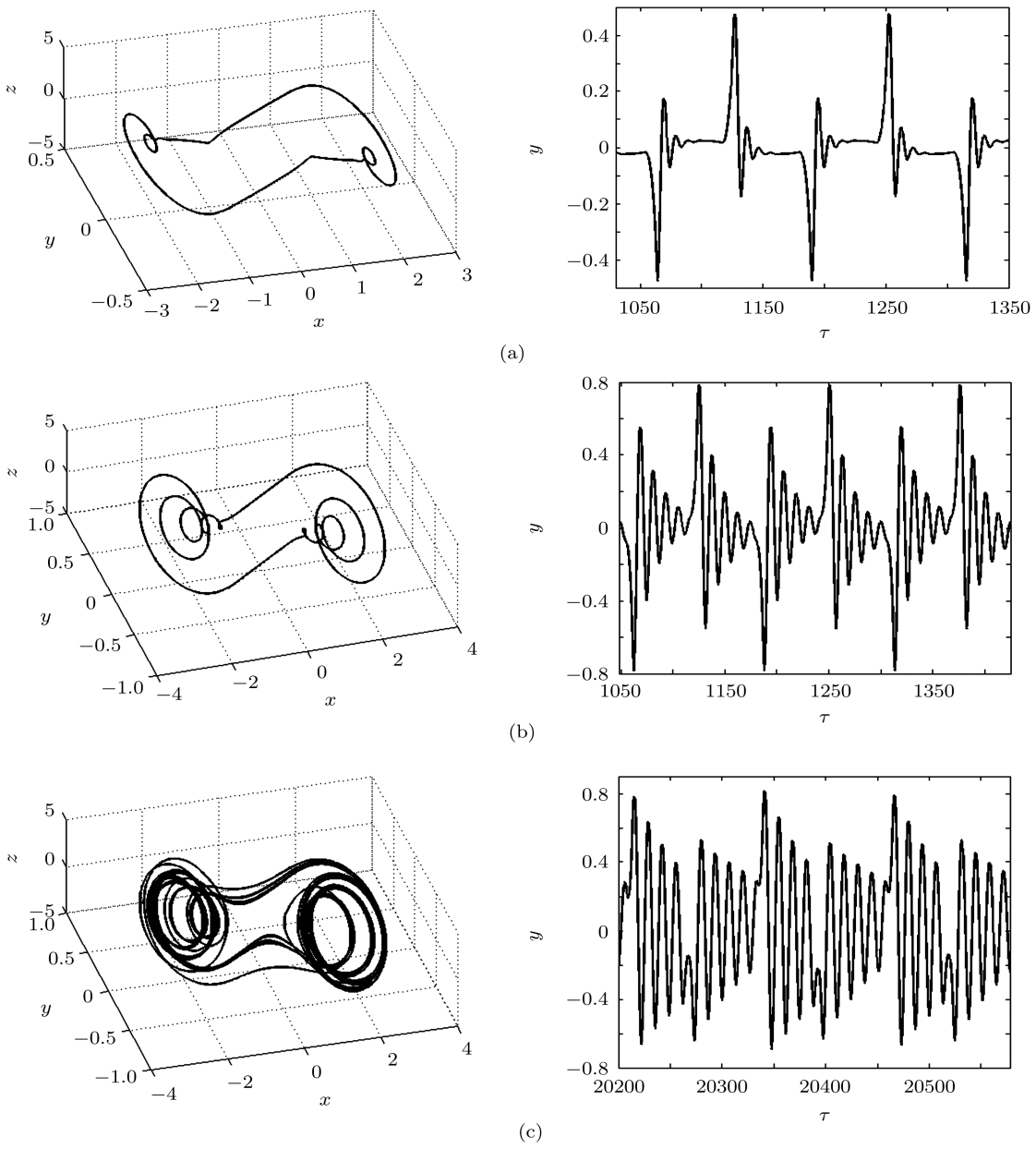


Fig. 4. Phase portraits and time variations of system (4) with different values of β : $\beta = 1.5$ (a), 1.1 (b), and 0.97 (c).

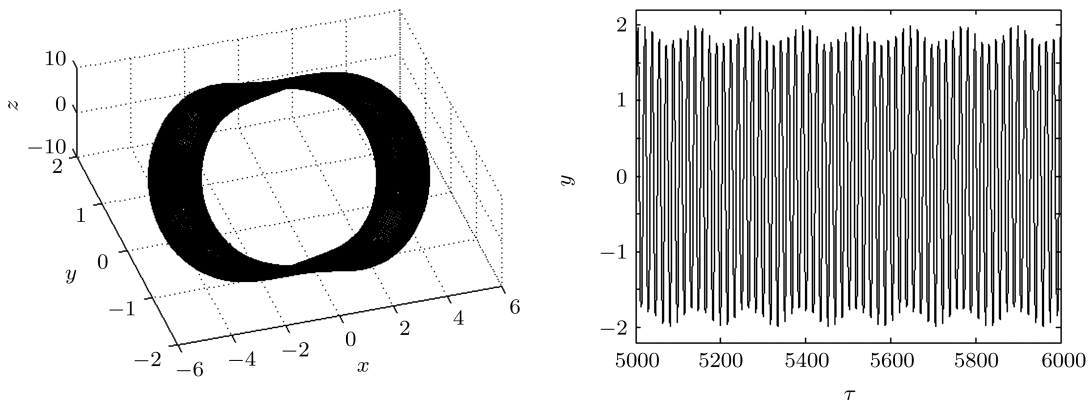


Fig. 5. Phase portrait and time variation of system (4) for $\beta = 0.96$.

Because there exists an order gap between the excitation frequency and the natural frequency of the system, dynamics may exhibit the fast–slow effect, which often behaves in a periodic state characterized by mixed mode oscillations. The type of oscillation, which has been observed in the numerical simulation for the circuit, can also be referred to as bursting phenomenon.[14] To reveal the mechanism of the movements is very important for understanding the complicated phenomena of the vector field. In the following, we will investigate the bifurcation details in the evolution of the dynamics.

4. Bifurcation mechanism

For the autonomous case with $I = 0$, Eq. (4) can be written in the following forms:

$$\frac{\mathrm{d}x}{\mathrm{d}\tau} = \alpha[y - x - k(x)],$$
$$\frac{\mathrm{d}y}{\mathrm{d}\tau} = x - y + z,$$
$$\frac{\mathrm{d}z}{\mathrm{d}\tau} = -\beta y, \tag{7}$$

where $k(x) = bx + \frac{1}{2}(a - b)(|x + 1| - |x - 1|)$, which has two switching boundaries: $\sum_1 = \{(x, y, z) \in R^3 | x = 1\}$ and $\sum_2 = \{(x, y, z) \in R^3 | x = -1\}$. The system has three equilibrium points expressed as

$P_0 : \{x = 0, y = 0, z = 0\}$ for $-1.0 < x < 1.0$,

$P_+ : \{x = -(a-b)/(1+b), y = 0, z = (a-b)/(1+b)\}$ for $x > 1.0$,

$P_- : \{x = (a-b)/(1+b), y = 0, z = -(a-b)/(1+b)\}$ for $x < -1.0$.

The equilibrium points as well as their properties depend on the special values of the parameters. For example, for the parameters fixed above, the details of the equilibriums can be computed as $P_0(x = 0, y = 0, z = 0)$ for $-1.0 < x < 1.0$, $P_+(x = 1.5, y = 0, z = -1.5)$ for $x > 1.0$ and $P_-(x = -1.5, y = 0, z = 1.5)$ for $x < -1.0$. When $\beta = 2.0$, the stabilities of P_0 and $P_\pm$ can be determined by the Jacobian matrix $\boldsymbol{J}_0$ with eigenvalues $\lambda^0_{1,2,3}$ and $\boldsymbol{J}_\pm$ with eigenvalues $\lambda^\pm_{1,2,3}$, respectively, where

$$\boldsymbol{J}_0 = \begin{pmatrix} 0.1429 & 1 & 0 \\ 1 & -1 & 1 \\ 0 & -2.0 & 0 \end{pmatrix}, \quad \lambda^0_1 = 0.2515, \lambda^0_{2,3} = -0.5543 \pm 0.9103\mathrm{i},$$

$$\boldsymbol{J}_\pm = \begin{pmatrix} -0.2857 & 1 & 0 \\ 1 & -1 & 1 \\ 0 & -2.0 & 0 \end{pmatrix}, \quad \lambda^\pm_1 = -0.6549, \lambda^\pm_{2,3} = -0.3154 \pm 0.8793\mathrm{i}.$$

Obviously, $P_\pm$ are asymptotically stable focal points, and P_0 is a saddle point. In order to explore the properties of the equilibrium points with the variation of parameter β, Table 1 gives the details of the eigenvalues associated with P_0 and $P_\pm$ with a few special values of β.

Table 1. Eigenvalues of linearized matrix associated with the equilibria.

	$-1.0 < x < 1.0$			$x > 1.0$ or $x < -1.0$	
$\beta = 1.5$	$\lambda^0_1 = 0.3026$,	$\lambda^0_{2,3} = -0.5799 \pm 0.6098\mathrm{i}$		$\lambda^\pm_1 = -0.9355$,	$\lambda^\pm_{2,3} = -0.1751 \pm 0.6538\mathrm{i}$
$\beta = 1.1$	$\lambda^0_1 = 0.3749$,	$\lambda^0_{2,3} = -0.6160 \pm 0.1990\mathrm{i}$		$\lambda^\pm_1 = -1.1841$,	$\lambda^\pm_{2,3} = -0.0508 \pm 0.5127\mathrm{i}$
$\beta = 0.97$	$\lambda^0_1 = 0.4065$,	$\lambda^0_2 = -0.8734$,	$\lambda^0_3 = -0.3903$	$\lambda^\pm_1 = -1.2576$,	$\lambda^\pm_{2,3} = -0.0141 \pm 0.4692\mathrm{i}$
$\beta = 0.96$	$\lambda^0_1 = 0.4091$,	$\lambda^0_2 = -0.8894$,	$\lambda^0_3 = -0.3769$	$\lambda^\pm_1 = -1.2631$,	$\lambda^\pm_{2,3} = -0.0113 \pm 0.4659\mathrm{i}$

Because the vector field is non-smooth but still continuous, we can use the generalized differential of Clarke to set up a generalized Jacobian matrix.[16] The generalised Jacobian matrix at the equilibrium points P_0 and $P_\pm$ for $\beta = 2.0$, expressed by the set-valued matrix $\boldsymbol{J}(\pm 1) = \{J_q, q \in [0, 1]\}$ with $J_q = qJ_0 + (1 - q)J_\pm$, at the bifurcation point is of the closed convex hull of the Jacobians on each side of the switching boundary.

Here we still take the case for $\beta = 2.0$ as an example to analyse the bifurcation mechanism. The three eigenvalues of $J(\pm 1)$ form three one-dimensional paths in the complex plane parameterised by the auxiliary variable q, denoted by $\lambda_i = \{\lambda_{qi}, q \in [0,1]\}$, for $i = 1,2,3$, where λ_{qi} are the eigenvalues of J_q. The paths of eigenvalues of the generalised Jacobian at $x = \pm 1.0$ are depicted in Fig. 6. One of eigenvalues of J_q is real number which crosses the imaginary axis at the origin for $q = 0.6667$ and the other two eigenvalues are a pair of conjugate complex numbers. The paths of the eigenvalues of $J(\pm 1)$ show that the discontinuous bifurcation point is a single crossing bifurcation,[17] in the sense that the eigenvalues cross the imaginary axis only once during their jump.

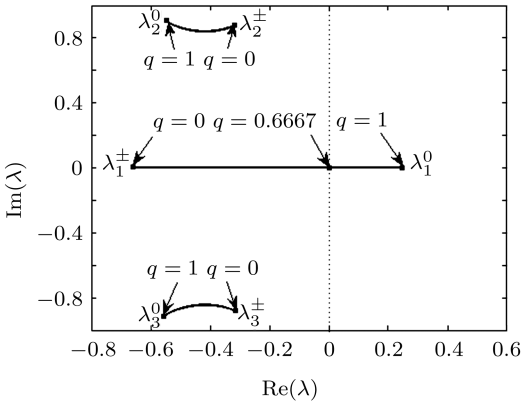


Fig. 6. Path of eigenvalues of generalised Jacobian.

We now turn to the non-autonomous case with $I \neq 0$, which implies that the dynamics of the circuit will be influenced by the external excitation. The excitation may cause the disappearance of the equilibria described above and drive the system to oscillate periodically according to the frequency of the excitation.

In order to conveniently describe the bifurcation mechanism, we introduce the transformation $\omega\tau = \theta$, and regard the dimensionless time τ as a variable parameter, which leads the vector field to be in the generalized 'autonomous' form and to be expressed as

$$\begin{aligned} \frac{\mathrm{d}x}{\mathrm{d}\tau} &= \alpha[y - x - k(x)] + I\cos\theta, \\ \frac{\mathrm{d}y}{\mathrm{d}\tau} &= x - y + z, \\ \frac{\mathrm{d}z}{\mathrm{d}\tau} &= -\beta y, \end{aligned} \tag{8}$$

where $k(x) = bx + \frac{1}{2}(a-b)(|x+1| - |x-1|)$.

Because of the linear structure of the circuit, though it is non-smooth, we can still assume the approximate solution to be in the following form:

$$\begin{aligned} x &= A_1\cos\theta + B_1\sin\theta + C_1, \\ y &= A_2\cos\theta + B_2\sin\theta + C_2, \\ z &= A_3\cos\theta + B_3\sin\theta + C_3. \end{aligned} \tag{9}$$

Substituting Eq. (9) into Eq. (8) yields the expressions of the coefficients in the approximate solution, the details of which are described as follows:

(1) for $x > 1.0$,

$$\begin{aligned} &A_1 = \alpha V(-2b\beta\omega^2 + b\omega^2 + b\omega^4 + b\beta^2 + \beta^2 - 2\beta\omega^2 + \omega^4)/H_{\pm}, \\ &B_1 = V\omega(-2\beta\omega^2 + \omega^2 + \omega^4 + \beta^2 - \beta\alpha + \alpha\omega^2)/H_{\pm}, \quad C_1 = (-a+b)/(b+1), \\ &A_2 = \omega^2 V(\beta - \omega^2 + \alpha b)/H_{\pm}, \quad B_2 = V(\omega^2 - \beta\alpha + \alpha\omega^2 - \beta\alpha b + b\alpha\omega^2)\omega/H_{\pm}, \\ &C_2 = 0, A_3 = \beta V(\omega^2 - \beta\alpha + \alpha\omega^2 - \beta\alpha b + b\alpha\omega^2)/H_{\pm}, \quad B_3 = -\omega\beta V(\beta - \omega^2 + \alpha b)/H_{\pm}, \\ &C_3 = -(-a+b)/(b+1); \end{aligned}$$

(2) for $-1.0 < x < 1.0$,

$$\begin{aligned} &A_1 = \alpha V(-2a\beta\omega^2 + a\omega^2 + a\omega^4 + a\beta^2 + \beta^2 - 2\beta\omega^2 + \omega^4)/H_0, \\ &B_1 = V\omega(-2\beta\omega^2 + \omega^2 + \omega^4 + \beta^2 - \beta\alpha + \alpha\omega^2)/H_0, \quad C_1 = 0, \\ &A_2 = \omega^2 V(\beta - \omega^2 + \alpha a)/H_0, \quad B_2 = V\omega(\omega^2 - \beta\alpha + \alpha\omega^2 - \beta\alpha a + a\alpha\omega^2)/H_0, C_2 = 0, \\ &A_3 = \beta V(\omega^2 - \beta\alpha + \alpha\omega^2 - \beta\alpha a + a\alpha\omega^2)/H_0, B_3 = -\omega\beta V(\beta - \omega^2 + \alpha a)/H_0, \quad C_3 = 0; \end{aligned}$$

(3) for $x < -1.0$,

$$\begin{aligned} &A_1 = \alpha V(-2b\beta\omega^2 + b\omega^2 + b\omega^4 + b\beta^2 + \beta^2 - 2\beta\omega^2 + \omega^4)/H_{\pm}, \\ &B_1 = V\omega(-2\beta\omega^2 + \omega^2 + \omega^4 + \beta^2 - \beta\alpha + \alpha\omega^2)/H_{\pm}, \quad C_1 = -(b-a)/(b+1), \end{aligned}$$

$$A_2 = \omega^2 V(\beta - \omega^2 + \alpha b)/H_\pm, \quad B_2 = V\omega(\omega^2 - \beta\alpha + \alpha\omega^2 - \beta\alpha b + b\alpha\omega^2)/H_\pm, \quad C_2 = 0,$$
$$A_3 = \beta V(\omega^2 - \beta\alpha + \alpha\omega^2 - \beta\alpha b + b\alpha\omega^2)/H_\pm, \quad B_3 = -\omega\beta V(\beta - \omega^2 + \alpha b)/H_\pm,$$
$$C_3 = (b-a)/(b+1),$$

where

$$\begin{aligned} H_0 =& -2\omega^4\beta + \omega^2\beta^2 + \omega^4 + \alpha^2\beta^2 + 2\omega^4\alpha + \omega^4\alpha^2 + \omega^6 + 2a\alpha^2\beta^2 + 2a\alpha^2\omega^4 - 2\omega^2\beta\alpha \\ & - 2\beta\alpha^2\omega^2 + a^2\alpha^2\omega^2 + a^2\alpha^2\omega^4 + a^2\alpha^2\beta^2 - 4a\alpha^2\beta\omega^2 - 2a^2\alpha^2\beta\omega^2, \\ H_\pm =& -2\omega^4\beta + \omega^2\beta^2 + 2b\alpha^2\beta^2 + 2b\alpha^2\omega^4 - 2\omega^2\beta\alpha - 2\beta\alpha^2\omega^2 + \omega^4 + \alpha^2\beta^2 + 2\omega^4\alpha \\ & + \omega^4\alpha^2 + \omega^6 - 4b\alpha^2\beta\omega^2 + b^2\alpha^2\omega^2 + b^2\alpha^2\omega^4 + b^2\alpha^2\beta^2 - 2b^2\alpha^2\beta\omega^2. \end{aligned}$$

Note that the 'solution', which is a periodically function of τ with period $T = 2\pi/\omega$, is not the real solution of the system. However, the type of the 'solution' can help us to understand the special behaviours of the system, the details of which are further discussed in the following.

The 'solution' in Eq. (9) can be regarded as a generalized equilibrium state, the stability of which can be determined by the eigenvalues associated with the linearized matrix of the vector field. Further computation reveals that these eigenvalues related to the 'solution' can be expressed in the same forms as those eigenvalues of the equilibrium points for the autonomous case because of the piecewise linear structure of the system. For example, when $\beta = 2.0$, while other parameters are still fixed at those values in Section 3, the 'solution' is a stable focus for $|x| > 1.0$ while a saddle point for $|x| < 1.0$.

Now we explain the mechanism of the periodic motion for the case $\beta = 2.0$ as an example. The 'solution' as well as the real solution is presented in Fig. 7. We set A_1 as the starting point, which is located at the switching boundary $\Sigma_1(\Sigma_1 = \{(x, y, z) \in R^3 | x = 1\})$. Because of the clockwise direction of the trajectory, which can be demonstrated by the time variation of y plotted in Fig. 3, the trajectory will tend to the stable focus with the natural angular frequency 0.8793 determined by the imaginary part of the complex eigenvalue for $|x| > 1.0$. The passage is relatively fast, called spiking (SP_1). When the trajectory meets the 'solution' at B_1, it may move exactly along the 'solution' with the excitation angular frequency $f = \omega = 0.05$ until it meets the switching boundary Σ_1. Note that the passage remaining on the 'solution' is relatively slow, which can be named quiescent state (QS_1).

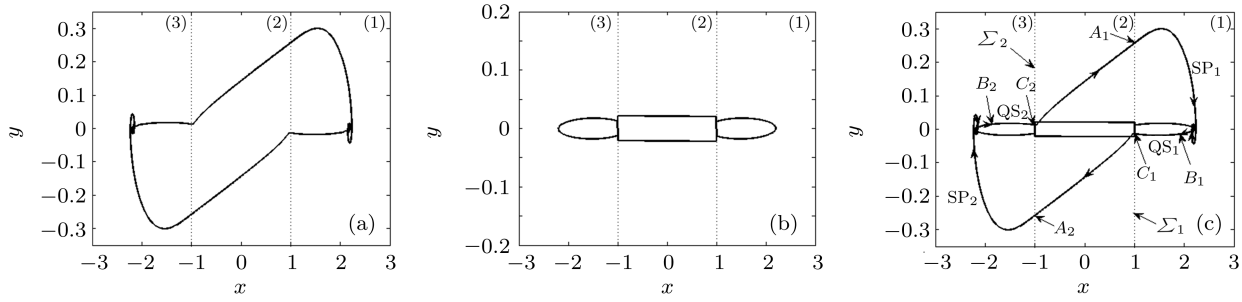


Fig. 7. (a) Real solution, (b) 'solution', where parts (1) and (3) denote the stable 'solutions' while part (2) denotes the unstable 'solutions', and (c) overlap of the 'solution' and the real solution.

Non-smooth bifurcation, i.e., the single crossing bifurcation, occurs when the trajectory crosses the switching boundary Σ_1 at the point C_1. Clearly, the behaviour of a single crossing bifurcation is present in the bifurcation scenario observed in Fig. 6.[16,17] Here the single crossing bifurcation leads to the instability of QS_1, resulting in another fast passage, i.e., spiking (SP_2). Because the 'solution' between the two switching boundary Σ_1 and $\Sigma_2(\Sigma_2 = \{(x, y, z) \in R^3 | x = -1\})$ is a saddle point

with one relatively large positive real eigenvalue, the trajectory will quickly move from the point C_1 to the switching Σ_2 boundary at A_2. Note that no bifurcation takes place at A_2. Because of the symmetric property of the 'solution', the behaviour of the trajectory from A_2 through B_2 to C_2 is similar to that of the trajectory from A_1 to C_1 described above. At the point C_2 on the switching boundary Σ_2, non-smooth bifurcation can be found, which changes the quiescent state (QS_2) into another repetitive spiking (SP_2), until the trajectory reaches the point A_1 and begins another period.

Now we turn to the complicated evolution of the dynamics with β value decreasing from 1.5 to 0.97. From the eigenvalues for some special values of β, presented in Table 1, one may find that the imaginary parts of the complex eigenvalues decrease slowly with the decrease of β, while the absolute values of real part of the complex eigenvalues decrease quickly, resulting in the rapid increase of the oscillating time in the spiking.

The periodic bursting bifurcates to quasi-periodic motion as β decreases to 0.9621. The behaviours of the quasi-periodic motion are strongly associated with the eigenvalues of the generalized Jacobian matrix. For example, when $\beta = 0.96$, computation reveals that one of the two frequencies of the quasi-periodic solution is the same as the frequency of the excitation, i.e., 0.05, while the other is near to the imaginary part of the complex eigenvalues, approximately at 0.4659.

5. Conclusions

For the double-scroll circuit with an order gap between the natural frequency and the excitation frequency, the fast–slow effect behaving in bursters can be observed. Non-smooth bifurcations at the switch boundaries connect the slow passage (quiescent states) and the fast passage (spiking states). By employing the generalized differential of Clarke in the linear form of solutions, it can be found that all the discontinuous bifurcations are related to the single cross of the imaginary axis. Further investigation reveals that both the imaginary parts and the real parts of the eigenvalues of the generalized matrix at the switch boundaries influence the structures of the phase portraits, and therefore affect the interaction process between the slow and fast passages.

References

[1] Wang L, Xu W and Li Y 2008 *Acta Phys. Sin.* **57** 6169

[2] Leine R I 2006 *Physica* D **223** 121

[3] Ugur Cam 2004 *Comput. Electrical Eng.* **30** 281

[4] Matsumoto T and Chua L O 1985 *IEEE Trans. Circuits and Systems, CAS* **32** 797

[5] Rene O Medrano-T, Murilo S Baptista and Ibere L Caldas 2003 *Physica* D **186** 133

[6] Zhang H B, Xia J W, Yu Y B and Dang C Y 2010 *Chin. Phys.* B **19** 030505-1

[7] Itoh M and Murakami H 1994 *Int. J. Bifur. and Chaos* **4** 1721

[8] Chen Z Y, Zhang X F and Bi Q S 2010 *Acta Phys. Sin.* **59** 2326 (in Chinese)

[9] Zhang X F, Chen Z Y and Bi Q S 2009 *Acta Phys. Sin.* **58** 2963 (in Chinese)

[10] Han X J, Jiang B and Bi Q S 2009 *Phys. Lett.* A **373** 3643

[11] Han X J, Jiang B and Bi Q S 2008 *Acta Phys. Sin.* **58** 6006

[12] Penney R W, Coolen A C C and Sherrington D 1993 *Journal of Physics* A: *Mathematical and General* **26** 3681

[13] Lisa Holden and Thomas Erneux 1993 *J. Math. Biol.* **31** 351

[14] Izhikevich E 2000 *Int. J. Bifurc. and Chaos* **6** 1171

[15] Ji Y and Bi Q S 2010 *Phys. Lett.* A **374** 1434

[16] Leine R I and van Campen D H 2006 *Eur. J. Mech. A Solids* **25** 595

[17] Leine R I, van Campen D H and Van de Vvrande B L 2000 *Nonlinear Dynamics* **23** 105